5th AIAA Theoretical Fluid Mechanics Conference
23 - 26 June 2008, Seattle, Washington

AIAA 2008-4227

Structural Sensitivity of Linear and Nonlinear Global Modes

P. Luchini * and F. Giannetti † and J. O. Pralits †

Universitá di Salerno, Fisciano (SA),84084, Italy

The concept of "structural sensitivity" of a global mode is introduced and used to study the formation of the classical Kármánvortex street in the wake of a circular cylinder. By evaluating the functional derivative of the global mode frequency with respect to an external local feedback from velocity to force, we show how to locate the "wavemaker" of the asymptotic theory, *i.e.*the point in space where the instability originates and from which propagates as a wave in all direction. This can be done by exploiting the properties of the numerically computed direct and adjoint global eigenfunctions, without any assumptions on the quasi-parallelism of the flow. This new approach is presented both in the context of linear as well nonlinear oscillations. Finally, recent results obtained by the application of the structural sensitivity concept to the study of the secondary instability of the cylinder wake are shown and discussed.

Downloaded by Gurlith Petersson on November 7, 2012 | http://arc.aiaa.org | DOI: 10.2514/6.2008-4227

Nomenclature

σ	Floquet exponent
κ	Spanwise wavenumber
T	Shedding period
Re	Reynolds number
St	Strouhal number
ω	Shedding frequency
$\mathbf{L}$	Linearised Navier-Stokes operator
$\mathbf{L}^+$	Adjoint Navier-Stokes operator
$\mathbf{u}$	Velocity vector
p	Reduced pressure
$\mathbf{f}^+$	Sensitivity to momentum forcing
m^+	Sensitivity to mass injection
$\mathbf{S}$	Sensitivity tensor
$\|\ \|_2$	Spectral norm
$\|\ \|$	Modulus of a complex number
Tr( )	Trace of a matrix

I. Introduction

In specific conditions, a large class of spatially developing flows sustain synchronised periodic oscillations over extended regions of the flow field, displaying an intrinsic dynamics characterised by a sharp frequency selection. The whole flow field behaves like a global oscillator and the structure underlying the spatial distribution of the fluctuations is usually termed "global mode". The asymptotic theoretical approach to global modes, initially formulated by Huerre & Monkewitz (1990)[1] and recently reviewed by Chomaz (2005),[2] takes life as an extension of the theory of absolute instabilities, introduced in the sixties in the context of plasma instabilities, to propagation media with slowly varying properties in space. Using a quasi-parallel

*Prof., Dipartimento di Ingegneria Meccanica, Via Ponte Don Melillo, AIAA Member 297010.
†Dr., Dipartimento di Ingegneria Meccanica, Via Ponte Don Melillo.

Copyright © 2008 by P. Luchini. Published by the American Institute of Aeronautics and Astronautics, Inc., with permission.

(WKBJ) approximation, at times pushed to the limits of its domain of applicability, this theory determines, in the absolutely unstable region, a specific point in space, possibly of complex coordinates, which acts as a "wavemaker" and from which the instability originates and propagates as a wave in all directions. The growth or damping rate of the wave at this particular point coincides with the global amplification or damping rate. For example, in a linear setting, the complex global frequency ω_g is obtained by the saddle-point condition

$$\omega_g = \omega_0(X_s) \quad \text{with} \quad \frac{\partial \omega_0}{\partial X}(X_s) = 0 \tag{1}$$

based on the analytic continuation of the local absolute frequency curve $\omega_0(X)$ in the complex X-plane, with X denoting here the slow streamwise variable. A result obtained by Giannetti & Luchini (2007),[3] was to link the originating point of the wave predicted by this theory with the behaviour of numerical simulations, in particular of the cylinder wake. The tool enabling this result was the "structural sensitivity" of the global mode, *i.e.*the functional derivative of its frequency with respect to an external local feedback from velocity to force, seen as a function of the point in space where the feedback is applied. This sensitivity can be computed numerically from direct and adjoint global modes without any assumption of local quasi-parallelism. The underlying rationale is that, if a part of the spatial range of the instability acts as the driving oscillator (wavemaker), and another part as an amplifier of these oscillations, the amplitude of the direct mode may well be larger in the amplifier, but the structural sensitivity will be largest where the oscillator resides. The concept of structural sensitivity makes perfect sense for nonlinear as well as linear oscillations. More recent work led us to computing the structural sensitivity of the finite-amplitude periodic cycle of the cylinder wake for supercritical Reynolds numbers, showing among other results that the mean-flow modification induced by a small perturbing body is responsible for a much larger effect than the direct influence of the perturbing body on the oscillation. Needless to say, that the structural stability analysis is also a very useful tool for the design of control systems. Here we will review the concept of "structural sensitivity" by applying it to a classical problem in hydrodynamics, namely the flow behind a circular cylinder. After presenting the results for the linear and nonlinear evolution of the vortex shedding we will introduce some recent development of the theory and show how a similar approach can also be used to study the characteristics of the secondary instability of the cylinder wake.

II. Problem formulation and governing equation

A classical example of fluid motion which, in a specific parameter range, behaves like a global oscillator is represented by the flow past an infinitely long circular cylinder. The steady two-dimensional symmetric flow existing at low Reynolds numbers becomes unstable when Re is increased beyond the critical value $Re_{c,1} \approx 47$ (Provansal *et al.* 1987).[4] The transition from steady to unsteady state occurs via a Hopf bifurcation (Noack & Eckelmann 1994[5]) which breaks the symmetry of the flow field and gives rise to a periodic self-sustained structure usually termed von Kármánvortex street. For Reynolds numbers lower than $Re_{c,2}$, where $189 \lesssim Re_{c,2} \lesssim 190$, the flow remains strictly two-dimensional (Barkley & Henderson 1996;[6] Williamson 1988,[7] 1996[8]) while for $Re > Re_{c,2}$ the flow becomes unstable to 3D perturbations and quickly evolves towards a complex three-dimensional state. The equations describing the motion of an incompressible fluid around an infinitely long cylinder are the classical incompressible Navier–Stokes equations

$$\frac{\partial \mathbf{U}}{\partial t} + \mathbf{U} \cdot \nabla \mathbf{U} = -\nabla P + \frac{1}{Re} \mathbf{\Delta U} \tag{2a}$$

$$\nabla \cdot \mathbf{U} = 0 \tag{2b}$$

where $\mathbf{U}$ is the velocity vector with components $\mathbf{U} = (U, V, W)$ and P is the reduced pressure. To set the notation, a Cartesian coordinate system is placed in the cylinder centre, with the x axis pointing in the flow direction and the z axis running along the cylinder centreline. Equations (2) are made dimensionless using the cylinder diameter D^* as the characteristic length scale, the velocity of the incoming uniform stream U^*_∞ as the reference velocity and $\rho^* U^{*2}_\infty$ as the reference pressure. The boundary conditions for the problem are the classical no-slip and no-penetration conditions on the surface of the cylinder together with the requirement that the flow approaches asymptotically the incoming uniform stream.

Downloaded by Gurlith Petersson on November 7, 2012 | http://arc.aiaa.org | DOI: 10.2514/6.2008-4227

Downloaded by Gurlith Petersson on November 7, 2012 | http://arc.aiaa.org | DOI: 10.2514/6.2008-4227

II.A. Linear Stability Analysis

The occurrence and the characteristics of the various instabilities of the cylinder wake at different Reynolds numbers can be studied through a linear stability analysis. The total field $\mathbf{Q} = \{\mathbf{U}, P\}$ is here decomposed into the sum of a two-dimensional base flow and a small unsteady perturbation as

$$\mathbf{U}(x,y,z,t) = \mathbf{U}_b(x,y,t) + \epsilon \frac{1}{\sqrt{2\pi}} \int_{-\infty}^{\infty} \mathbf{u}(x,y,\kappa,t)) \ \exp(\mathrm{i}\kappa z)\mathrm{d}\kappa \tag{3a}$$

$$P(x,y,z,t) = P_b(x,y,t) + \epsilon \frac{1}{\sqrt{2\pi}} \int_{-\infty}^{\infty} p(x,y,\kappa,t) \ \exp(\mathrm{i}\kappa z)\mathrm{d}\kappa \tag{3b}$$

where the amplitude ϵ is assumed small and a Fourier transform is used to express the span-wise dependence of a general three-dimensional perturbation. Such decomposition can be used to study both the stability of the stationary base flow which exists for $Re <= Re_{c,1}$ and of the periodic Kármánstreet which persists in the range $Re_{c,1} < Re < Re_{c,2}$. Note in fact that any steady field can be viewed as a particular case of a periodic field for which the period is infinite. Thus, for sake of generality, it is convenient here to derive the results for a two-dimensional periodic base flow $\mathbf{Q}_b(x,y,t) = \mathbf{Q}_b(x,y,t+T)$ and use more restrictive assumptions only when specifically required. Introducing (3) in (2) and linearising, we obtain two problems describing respectively the evolution of the two-dimensional base flow and the development of the three-dimensional perturbation. In particular the base flow is governed by the two-dimensional version of (2), while the perturbed field is described by the following set of linearised unsteady Navier–Stokes equations (LNSE)

$$\frac{\partial \mathbf{u}}{\partial t} + \mathbf{L}_\kappa\{\mathbf{U}_b, Re\}\mathbf{u} = -\nabla_\kappa p \tag{4a}$$

$$\nabla_\kappa \cdot \mathbf{u} = 0 \quad . \tag{4b}$$

In the above expressions $\nabla_\kappa \equiv (\frac{\partial}{\partial x}, \frac{\partial}{\partial x}, \mathrm{i}\kappa)$ is the modified gradient operator and $\mathbf{L}_\kappa$ stands for the modified three-dimensional linearised Navier–Stokes operator which in vector notation can be written as

$$\mathbf{L}_\kappa\{\mathbf{U}_b, Re\}\mathbf{u} = \mathbf{U}_b \cdot \nabla_\kappa \mathbf{u} + \mathbf{u} \cdot \nabla_\kappa \mathbf{U}_b - \frac{1}{Re}\mathbf{\Delta}_\kappa \mathbf{u} \ , \tag{5}$$

where $\mathbf{\Delta}_\kappa \equiv \nabla_\kappa \cdot \nabla_\kappa$ is the modified Laplacian operator. Note that for $\kappa = 0$ the spanwise component of the momentum equation is decoupled and reduces to a simple convection-diffusion equation: this implies that in these circumstances the stability of the flow can be studied trough a pure two-dimensional analysis. In such cases, to simplify the presentation, we will neglect the subscript κ, intending in this way the two-dimensional version of the equations. To perform a stability analysis equations (5) must be supplemented with homogeneous boundary conditions on the surface of the cylinder and in the far field. In order to determine the time asymptotic behaviour of (4) it is convenient to adopt a normal mode expansion. In particular, for a given value of κ, we will look for Floquet modes, *i.e.*solutions of the homogeneous Linearised Navier–Stokes equations (4) of the form

$$\mathbf{u}(x,y,\kappa,t) = \hat{\mathbf{u}}(x,y,\kappa,t) \ \exp(\sigma t) \tag{6a}$$

$$p(x,y,\kappa,t) = \hat{p}(x,y,\kappa,t) \ \exp(\sigma t) \ . \tag{6b}$$

Here σ is the Floquet exponent, i.e. the eigenvalue of the Floquet transition operator, while $\hat{\mathbf{q}} = \{\hat{\mathbf{u}}, \hat{p}\}$ is a non trivial periodic complex field

$$\hat{\mathbf{q}}(x,y,\kappa,t+T) = \hat{\mathbf{q}}(x,y,\kappa,t) \tag{7}$$

satisfying equations

$$\frac{\partial \hat{\mathbf{u}}}{\partial t} + \sigma\hat{\mathbf{u}} + \mathbf{L}_\kappa\{\mathbf{U}_b, Re\}\hat{\mathbf{u}} + \nabla\hat{p} = \mathbf{0} \tag{8a}$$

$$\nabla \cdot \hat{\mathbf{u}} = 0 \tag{8b}$$

along with homogeneous boundary conditions on the cylinder surface and appropriate far-field radiation conditions. Note that if the base flow is steady, $\hat{\mathbf{q}}$ does not depend on time and consequently the temporal derivative in (8) drops out. The system of equations (8) along with its boundary conditions in space and the condition (7) in time represents an eigenvalue problem for σ. For $\mathrm{Re}(\sigma) < 0$ the flow is stable while for $\mathrm{Re}(\sigma) > 0$ the mode is unstable and the perturbation grows exponentially in time until nonlinear effects become important.

II.B. Adjoint Equations

An important concept, strictly related to the notion of"structural sensitivity", is that of adjoint of a differential operator. For any pair of suitably differentiable fields $\mathbf{q} \equiv \{\mathbf{u}, p\}$ and $\mathbf{g}^+ \equiv \{\mathbf{f}^+, m^+\}$, which do not have to satisfy equations (4), the following Lagrange identity is constructed using differentiation by parts

$$\left[\left(\frac{\partial \mathbf{u}}{\partial t} + \mathbf{L}_\kappa\{\mathbf{U}_b, Re\}\mathbf{u} + \nabla_\kappa p\right)\cdot \mathbf{f}^+ + (\nabla_\kappa \cdot \mathbf{u})\ \hat{m}^+\right] + \left[\mathbf{u}\cdot\left(\frac{\partial \mathbf{f}^+}{\partial t} + \mathbf{L}_\kappa^+\{\mathbf{U}_b, Re\}\mathbf{f}^+ + \nabla_\kappa m^+\right) + p\ \left(\nabla_\kappa \cdot \mathbf{f}^+\right)\right] = \frac{\partial \mathbf{u}\cdot\mathbf{f}^+}{\partial t} + \nabla_\kappa \cdot \mathbf{J}_\kappa(\mathbf{q}, \mathbf{g}^+) \quad . \tag{9}$$

In the above expression $\mathbf{J}(\mathbf{q}, \mathbf{g}^+)$ is the "bilinear concomitant"

$$\mathbf{J}_\kappa(\mathbf{q}, \mathbf{g}^+) = \mathbf{U}_b(\mathbf{u}\cdot\mathbf{f}^+) + \frac{1}{Re}\left(\nabla_\kappa \mathbf{f}^+ \cdot \mathbf{u} - \nabla_\kappa \mathbf{u}\cdot\mathbf{f}^+\right) + m^+\ \mathbf{u} + p\ \mathbf{f}^+ \tag{10}$$

and $\mathbf{L}_\kappa^+$ is the adjoint linearised Navier–Stokes operator which in vector notation can be expressed as

$$\mathbf{L}_\kappa^+\{\mathbf{U}_b, Re\}\mathbf{f}^+ = \mathbf{U}_b \cdot \nabla_\kappa \mathbf{f}^+ - \nabla_\kappa \mathbf{U}_b \cdot \mathbf{f}^+ + \frac{1}{Re}\boldsymbol{\Delta}_\kappa \mathbf{f}^+. \tag{11}$$

Integration over space and time of (9) and use of the divergence theorem gives the generalised Green's theorem for the LNSE. Examining the second term in the square brackets on the left hand side of the Lagrange identity (9) we define the adjoint equations as

$$\frac{\partial \mathbf{f}^+}{\partial t} + \mathbf{L}_\kappa^+\{\mathbf{U}_b, Re\}\mathbf{f}^+ + \nabla_\kappa m^+ = \mathbf{0} \tag{12a}$$

$$\nabla_\kappa \cdot \mathbf{f}^+ = 0 \quad . \tag{12b}$$

It is through judicious manipulation of the right hand side of (9) that engenders the usefulness of the adjoint solutions $\mathbf{g}^+ = \{\mathbf{f}^+, m^+\}$. In particular for stability and receptivity considerations we are interested in the Floquet adjoint modes, i.e. non trivial solutions of the adjoint linearised Navier–Stokes equations (12) of the form

$$\mathbf{f}^+(x, y, \kappa, t) = \hat{\mathbf{f}}^+(x, y, \kappa, t)\ \exp(-\sigma t) \tag{13a}$$

$$m^+(x, y, \kappa, t) = \hat{m}^+(x, y, \kappa, t)\ \exp(-\sigma t) \quad . \tag{13b}$$

More specifically for a given value of κ, if $\mathbf{q}(x, y, \kappa, t) = \hat{\mathbf{q}}(x, y, \kappa, t)\exp(\sigma t)$ is the Floquet mode of the LNSE corresponding to the exponent σ, we define $\mathbf{g}^+(x, y, \kappa, t) = \hat{\mathbf{g}}^+(x, y, \kappa, t)\exp(-\sigma t)$ its adjoint mode if the complex field $\hat{\mathbf{g}}^+ = \{\hat{\mathbf{f}}^+, \hat{m}^+\}$ is a non trivial periodic solution

$$\hat{\mathbf{g}}^+(x, y, \kappa, t + T) = \hat{\mathbf{g}}^+(x, y, \kappa, t) \tag{14}$$

of equations

$$\frac{\partial \hat{\mathbf{f}}^+}{\partial t} - \sigma\ \hat{\mathbf{f}}^+ + \mathbf{L}_\kappa^+\{\mathbf{U}_b, Re\}\hat{\mathbf{f}}^+ + \nabla_\kappa \hat{m}^+ = \mathbf{0} \tag{15a}$$

$$\nabla_\kappa \cdot \hat{\mathbf{f}}^+ = 0 \tag{15b}$$

along with homogeneous boundary conditions on the cylinder surface and appropriate radiation conditions in the far field. As for the direct mode, if the base flow is stationary, the field $\hat{\mathbf{g}}^+$ does not depend on time and consequently the temporal derivative in equation (15) drops out.

Downloaded by Gurlith Petersson on November 7, 2012 | http://arc.aiaa.org | DOI: 10.2514/6.2008-4227

III. Structural sensitivity to spatially localised feedbacks

In order to study the self-exciting mechanism which gives rise to the vortex shedding at $Re = Re_{c,1} \approx 47$ or the characteristics of the secondary instability which develops for $Re > Re_{c,2} \approx 189$ it is useful to introduce the concept of *structural sensitivity*. In order to explain this notion, let us consider a perturbation in the structure of the eigenvalue problem (8) and consider the Floquet mode

$$\delta\mathbf{q}'(x,y,\kappa,t) = \delta\hat{\mathbf{q}}'(x,y,\kappa,t)\exp(\sigma' t) \tag{16}$$

which is the solution of the perturbed problem

$$\frac{\partial\hat{\mathbf{u}}'}{\partial t} + \sigma'\hat{\mathbf{u}}' + \mathbf{L}_\kappa\{\mathbf{U}_b, Re\}\hat{\mathbf{u}}' + \nabla_\kappa\hat{p}' = \delta\mathbf{H}(\hat{\mathbf{u}}', \hat{p}') \tag{17a}$$

$$\nabla_\kappa \cdot \hat{\mathbf{u}}' = \delta R(\hat{\mathbf{u}}', \hat{p}') \tag{17b}$$

along with the appropriate boundary conditions in space and the periodic condition

$$\hat{\mathbf{q}}'(x,y,\kappa,t+T) = \hat{\mathbf{q}}'(x,y,\kappa,t) \tag{18}$$

in time. Here $\delta\mathbf{H}$ and $\delta\mathbf{R}$ denote two linear differential operators expressing the structural perturbation of the original differential problem. The drift $\delta\sigma$ of the Floquet exponent and the mode perturbation $\delta\hat{\mathbf{q}} \equiv \{\delta\hat{\mathbf{u}}, \delta\hat{p}\}$ caused by the structural perturbation can be related using a simple expansion in terms of the solution of the unperturbed problem. Assuming $\hat{\mathbf{u}}' = \hat{\mathbf{u}} + \delta\hat{\mathbf{u}}$, $\hat{p}' = \hat{p} + \delta\hat{p}'$ and $\sigma' = \sigma + \delta\sigma$, inserting in (17) and neglecting quadratic terms, we easily obtain

$$\frac{\partial\delta\hat{\mathbf{u}}}{\partial t} + \sigma\ \delta\hat{\mathbf{u}} + \mathbf{L}_\kappa\{\mathbf{U}_b, Re\}\ \delta\hat{\mathbf{u}} + \nabla_\kappa\ \delta\hat{p} = -\delta\sigma\ \hat{\mathbf{u}} + \delta\mathbf{H}(\hat{\mathbf{u}}, \hat{p}) \tag{19a}$$

$$\nabla_\kappa \cdot\ \delta\hat{\mathbf{u}} = \delta R(\hat{\mathbf{u}}, \hat{p})\ . \tag{19b}$$

Multiplying this expression by $\exp(\sigma t)$ and introducing the field

$$\delta\mathbf{q}(x,y,\kappa,t) = \delta\hat{\mathbf{q}}(x,y,\kappa,t)\exp(\sigma t)\ , \tag{20}$$

equation (19) can be recast as

$$\frac{\partial\delta\mathbf{u}}{\partial t} + \mathbf{L}_\kappa\{\mathbf{U}_b, Re\}\ \delta\mathbf{u} + \nabla_\kappa\ \delta p = -\delta\sigma\ \mathbf{u} + \delta\mathbf{H}(\mathbf{u}, p) \tag{21a}$$

$$\nabla_\kappa \cdot\ \delta\mathbf{u} = \delta R(\mathbf{u}, p)\ . \tag{21b}$$

If we just wanted to determine the variation of the Floquet exponent for a specific form of the structural perturbation we could solve the problem as stated above; but we can obtain a much more powerful result, *i.e.* the sensitivity of the eigenvalue σ to an *arbitrary* structural perturbation with the aid of adjoint equations. Applying the Lagrange identity to the field $\delta\mathbf{q}$ (20) and to the adjoint Floquet mode $\mathbf{g}^+(x,y,t) = \hat{\mathbf{g}}^+(x,y,t)\exp(-\sigma t)$ corresponding to the eigenvalue σ, integrating in time over a period and in space over the spatial domain $\mathcal{D}$, we obtain

$$\begin{aligned}\int_t^{t+T}\int_{\mathcal{D}}\left(\frac{\partial\delta\mathbf{u}}{\partial t} + \mathbf{L}_\kappa\{\mathbf{U}_b, Re\}\delta\mathbf{u} + \nabla_\kappa\delta p\right)\cdot\mathbf{f}^+ + (\nabla_\kappa\cdot\delta\mathbf{u})\ \hat{m}^+\ \mathrm{d}^2\mathbf{x}\ \mathrm{d}t + \\ \int_t^{t+T}\int_{\mathcal{D}}\delta\mathbf{u}\cdot\left(\frac{\partial\mathbf{f}^+}{\partial t} + \mathbf{L}_\kappa^+\{\mathbf{U}_b, Re\}\mathbf{f}^+ + \nabla_\kappa m^+\right) + \delta p\ \left(\nabla_\kappa\cdot\mathbf{f}^+\right)\ \mathrm{d}^2\mathbf{x}\ \mathrm{d}t = \\ \int_t^{t+T}\int_{\mathcal{D}}\frac{\partial\delta\mathbf{u}\cdot\mathbf{f}^+}{\partial t}\ \mathrm{d}^2\mathbf{x}\ \mathrm{d}t\ +\ \int_t^{t+T}\oint_{\partial\mathcal{D}}\mathbf{J}(\delta\mathbf{q}, \mathbf{g}^+)\cdot\mathrm{d}\mathbf{l}\ \mathrm{d}t\quad .\end{aligned} \tag{22}$$

Assuming now that both the solution of equation (21) and the adjoint mode decay in the far field and taking advantage of the periodicity of $\delta\hat{\mathbf{q}}$ and $\hat{\mathbf{q}}^+$, we easily realize that the two terms on the right hand sides of (22) vanish. Since the adjoint mode satisfies equations (12) and equation (19) holds, we can further simplify (22) arriving at the following expression for the eigenvalue drift

Downloaded by Gurlith Petersson on November 7, 2012 | http://arc.aiaa.org | DOI: 10.2514/6.2008-4227

$$\delta\sigma = \frac{\displaystyle\int_t^{t+T}\int_D \mathbf{f}^+ \cdot \delta\mathbf{H}(\mathbf{u},p) + m^+\ \delta R(\mathbf{u},p)\ \mathrm{d}^2\mathbf{x}\ \mathrm{d}t}{\displaystyle\int_t^{t+T}\int_{\mathcal{D}} \mathbf{f}^+ \cdot \mathbf{u}\ \mathrm{d}^2\mathbf{x}\ \mathrm{d}t}. \tag{23}$$

Expression (23) is valid for a generic structural perturbation: the associated shift in the eigenvalue can be calculated once the operators $\delta\mathbf{H}$ and δR are specified. Equation (23) can be simplified if we consider structural perturbations localised in space. Consider for example the effects induced by the existence of a spatially localised feedback. More precisely let us consider the sensitivity of the Floquet exponent $\delta\sigma$ to a generic force-velocity coupling. In a linear theory approach the feedback process can be mathematically described by the following linear relation between force and velocity

$$\delta\mathbf{H} = \mathbf{C}(x,y,\kappa)\ \hat{\mathbf{u}}\ . \tag{24}$$

Here $\mathbf{C}$ denotes the matrix of the coupling coefficients which in general may be functions of the spatial coordinates (x,y). If the feedback is localised in space, however, we can simplify the model by assuming

$$\mathbf{C}(x,y\kappa) = \delta(x-x_0,y-y_0)\ \mathbf{C}_0(\kappa) \quad , \tag{25}$$

where $\mathbf{C}_0$ is now a constant coefficient matrix (for a given value of κ), (x_0,y_0) indicates the position where the feedback acts and $\delta(x-x_0,y-y_0)$ denotes the Kronecker delta function. In this case the Floquet exponent drift can be derived by taking $\delta\mathbf{H}(\mathbf{u},p) = \mathbf{C}(x,y,\kappa)\ \mathbf{u}$ and $\delta R(\mathbf{u},p) = 0$ in (23). In this way, using (25), we easily obtain

$$\delta\sigma = \frac{\displaystyle\int_t^{t+T}\int_D \hat{\mathbf{f}}^+ \cdot \mathbf{C}(x,y) \cdot \hat{\mathbf{u}}\ \mathrm{d}^2\mathbf{x}\ \mathrm{d}t}{\displaystyle\int_t^{t+T}\int_{\mathcal{D}} \hat{\mathbf{f}}^+ \cdot \hat{\mathbf{u}}\ \mathrm{d}^2\mathbf{x}\ \mathrm{d}t} = \mathbf{S}(x_0,y_0) : \mathbf{C}_0 = \sum_{ij} S_{ij}(x_0,y_0)\ C_{0ij} \tag{26}$$

where we have defined the sensitivity $\mathbf{S}$ as

$$\mathbf{S}(x,y) = \frac{\delta\sigma}{\delta\mathbf{C}_0} = \frac{\displaystyle\int_t^{t+T} \hat{\mathbf{u}}(x,y,\kappa,t)\ \hat{\mathbf{f}}^+(x,y,\kappa,t)\ \mathrm{d}t}{\displaystyle\int_t^{t+T}\int_{\mathcal{D}} \hat{\mathbf{f}}^+ \cdot \hat{\mathbf{u}}\ \mathrm{d}^2\mathbf{x}\ \mathrm{d}t} \quad . \tag{27}$$

In the above expressions the notation $\hat{\mathbf{u}}\ \hat{\mathbf{f}}^+$ indicates the dyadic product between the direct and adjoint Floquet modes. Notice that $\mathbf{C}_0$ is a tensor quantity, relating a force to a velocity, and so is $\mathbf{S}$. In the next sections we will show how the information contained in the sensitivity tensor can be used to study the characteristics and the development of the instabilities occurring in the wakes of bluff bodies.

IV. Structural sensitivity of the first instability of the cylinder wake

The theory developed in the previous section was initially introduced in a more simple setting by Giannetti & Luchini (2007) who studied the first instability of the cylinder wake. This occurs for two-dimensional perturbations ($\kappa = 0$) at $Re = Re_{c,1} \approx 47$. Giannetti & Luchini (2007)[3] determined numerically the steady symmetric solution of the Navier-Stokes and studied its stability characteristics by performing a two-dimensional global stability analysis. The direct and adjoint global modes were determined numerically through the use of an inverse iteration algorithm. As an example figure 1 shows the modulus of the velocity of the direct mode and its receptivity to momentum forcing at $Re = 50$ (i.e. the modulus of the adjoint field $\hat{\mathbf{f}}^+$).

It is interesting to note that the maxima of the direct mode are located far downstream of the recirculating region (the white line in the figures) while the regions of maximum receptivity to momentum forcing and mass injection (not shown here) are localised in the near wake of the cylinder, close to separation points. This large spatial separation is a characteristic of non-normal operators (Chomaz 2005).[2] Locating the zones where the maximum receptivity is attained it is however not sufficient to analyse the process which gives rise

Downloaded by Gurlith Petersson on November 7, 2012 | http://arc.aiaa.org | DOI: 10.2514/6.2008-4227

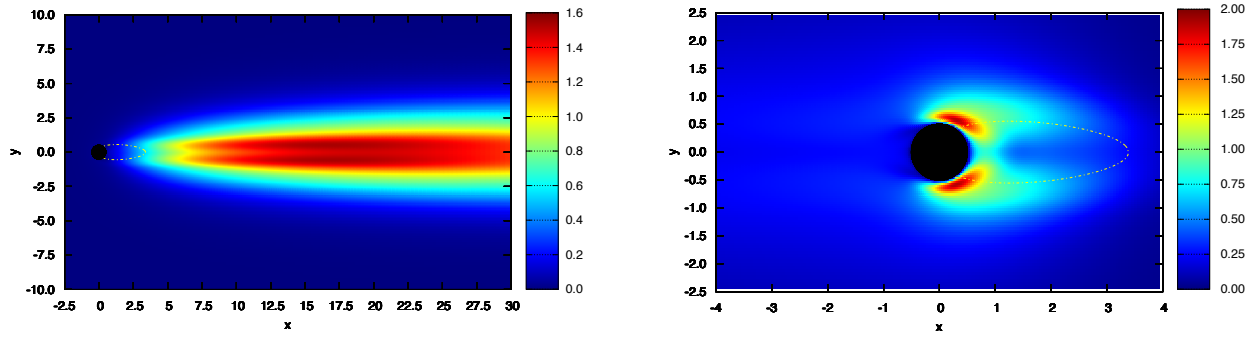

(a) (b)

Figure 1. (a) Spatial distribution of the velocity field modulus $\|\hat{\mathbf{u}}(x,y)\|$ at $Re = 50$. (b) Receptivity to momentum forcing and initial conditions ($\|\hat{\mathbf{f}}^+(x,y)\|$) at $Re = 50$.

to the von Kármán street. The vortex shedding behind bluff bodies, in fact, is generated by a self-exciting mechanism which needs a different approach to be fully understood. In the context of slowly evolving media, for example, the asymptotic theory developed by Chomaz *et al.* (1991),[9] Monkewitz *et al.* (1993)[10] and Le Dizès *et al.* (1996)[11] endows the region around the saddle point with the fundamental role of "*wavemaker*" in the excitation of the global mode. In the context of a two-dimensional modal analysis Giannetti & Luchini (2007)[3] introduced a concept similar to that of "wavemaker" by investigating where in space a modification in the structure of the problem is able to produce the greatest drift of the eigenvalue. This being the case, in fact, it would be justified to claim that the structural perturbation has hit the "core" of the instability mechanism. More precisely, they investigated the sensitivity of the eigenvalue $\delta\sigma$ with respect to a generic force-velocity coupling. Such a feedback could be in theory produced by introducing in the flow field a small device which exerts on the fluid a force whose direction and strength depend on the local value of the velocity perturbation. In a sense, a similar mechanism can be considered as the "wavemaker" of the asymptotic theory.

For a steady base flow, equation (27) simplifies to

$$\mathbf{S}(x,y) = \frac{\hat{\mathbf{f}}^+(x,y)\ \hat{\mathbf{u}}(x,y)}{\displaystyle\int_{\mathcal{D}} \hat{\mathbf{f}}^+ \cdot \hat{\mathbf{u}}\ \mathrm{d}^2\mathbf{x}} \quad . \tag{28}$$

since the direct and adjoint modes $\hat{\mathbf{q}} = \{\hat{\mathbf{u}}, \hat{p}\}$ and $\hat{\mathbf{g}}^+ = \{\hat{\mathbf{f}}^+, \hat{m}^+\}$ satisfying respectively equations (8) and (15) do not depend on time. The information contained in the tensor $\mathbf{S}(x,y)$ can be used to build a spatial sensitivity map. By looking for regions where the sensitivity is high, Giannetti & Luchini (2007)[3] determined the core of the instability, identifying, in this way, the *wavemaker* of the asymptotic theory. Since $\mathbf{S}$ is a tensor, various quantities may be chosen to represent the sensitivity. As an example figure 2 shows the spatial map obtained at $Re = 50$ by taking at each point in space the spectral norm of $\mathbf{S}$. This quantity represents the receptivity to spatially localised feedbacks due to a local force proportional to a local velocity of the worst possible direction. Other choices can be the Frobenius norm (sum of the squares of all four components) or the modulus of the trace (sensitivity to a force locally aligned with velocity, *i.e.* a pure resistance). This last quantity for example is shown in figure 3. Both maps show that large values of the sensitivity are attained in two lobes located symmetrically across the separation bubble. Note that both close to the cylinder and far from it the product of the adjoint and direct modes is small. This shows that these areas of the flow are not really important for the instability dynamics.

IV.A. Sensitivity of the eigenvalue to the size of the computational domain

The spatial distribution of the product between the direct and adjoint eigenfunctions suggests that the characteristics of the global mode are dictated mainly by the conditions existing in the region where the

Downloaded by Gurlith Petersson on November 7, 2012 | http://arc.aiaa.org | DOI: 10.2514/6.2008-4227

Downloaded by Gurlith Petersson on November 7, 2012 | http://arc.aiaa.org | DOI: 10.2514/6.2008-4227

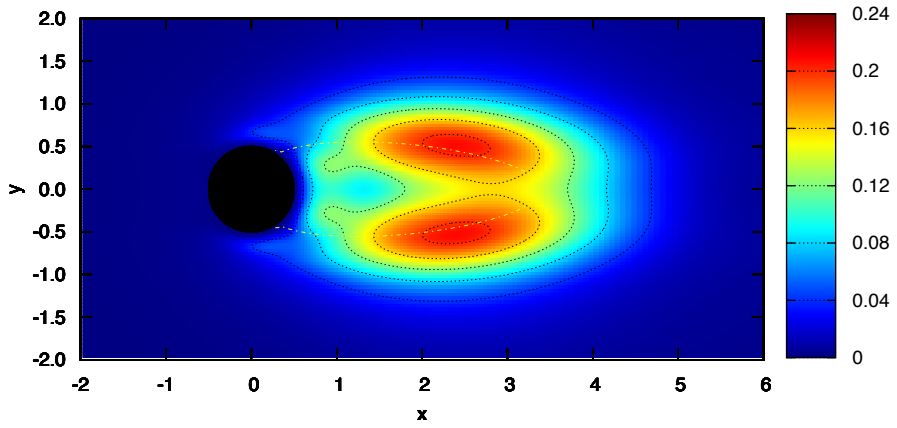

Figure 2. Receptivity to spatially localised feedbacks at $Re = 50$ due to local force proportional to a local velocity of the worst possible direction ($\|\mathbf{S}\|_2$)

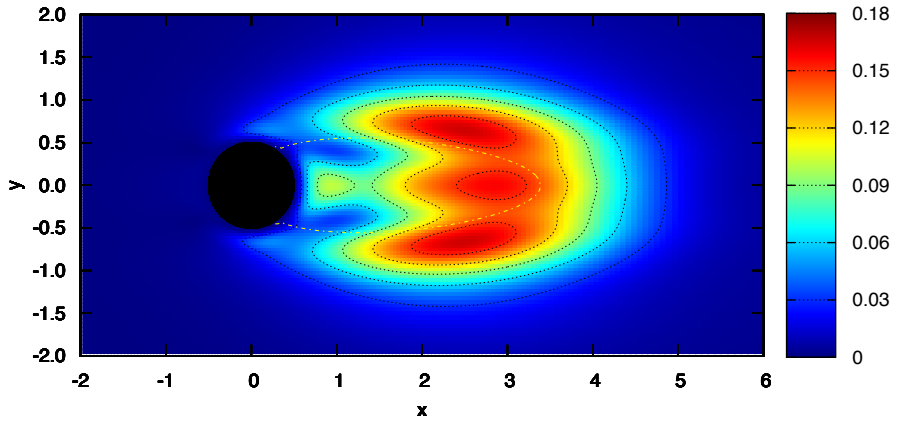

Figure 3. Receptivity to spatially localised feedbacks at $Re = 50$ due to local force proportional to a local velocity of the same direction (Modulus of the trace of $|\mathrm{Tr}(\mathbf{S})|$)

value of $\|\mathbf{S}\|_2$ is sufficiently large. In order to check this hypothesis, Giannetti & Luchini (2007)[3] repeated the stability analysis on progressively shortened domains in order to verify the influence of the different regions of the flow on the eigenvalue. Note that the problem of determining the sensitivity of σ to the size of the computational domain naturally fits in a structural stability framework: resizing the domain, in fact, is substantially equivalent to changing the boundary conditions of the discretized problem. The numerical

results showed excellent agreement with the predictions based on the spatial map displayed in figure 2. The analysis showed that the eigenvalue varies significantly only when the boundary conditions are placed in proximity of the regions in which the sensitivity is significantly different from zero. Until the instability core was not included inside the computational boundaries the eigenvalue drift remained relatively small. The spatial structure of the mode was also substantially preserved. As expected, imposing the inflow conditions near the cylinder surface was less effective than setting the outflow boundary across the separation bubble. Even when the cylinder was excluded from the computational domain a reasonable value for σ was found. A similar behaviour was also noticed by Triantafyllou & Karniadakis (1990)[12] who numerically reproduced a vortex street by using a computational domain restricted to the region downstream of the obstacle. All these results show that the core of the instability is located behind the cylinder, almost at the end of the recirculating region.

V. Analysis of the finite-amplitude periodic vortex shedding

From a theoretical point of view the approach introduced by Giannetti & Luchini (2007),[3] which is based on the properties of the steady base flow, is only valid in a neighbourhood of the neutral point. For $Re > Re_{c,1}$, in fact, the steady symmetric flow becomes unstable and a Kármánvortex street develops. In such conditions, after an initial transient, the flow becomes periodic

$$\mathbf{U}(x,y,t+T) = \mathbf{U}(x,y,t)\ ,\ \ P(x,y,t+T) = P(x,y,t) \tag{29}$$

with period T, Strouhal number $St = 1/T$ and angular pulsation $\omega = 2\pi/T$. Giannetti, Pralits & Luchini (2007)[13] and Luchini, Pralits & Giannetti (2008)[14] have extended the approach described in the previous section to study finite-amplitude vortex shedding, in order to assess how unsteadiness and saturation can modify the results obtained in the neighbourhood of the critical Reynolds number.

As described in the previous section, in order to locate the *wavemaker* of the instability, Giannetti & Luchini (2007)[3] determined the space distribution of the sensitivity of the eigenvalue to a structural perturbation of the problem. The analogous quantity for the nonlinear periodic oscillation is the space distribution of the sensitivity of its frequency to a structural perturbation of the problem. Suppose, therefore, to give a structural perturbation directly to the nonlinear two-dimensional equations (2), in the form of a body force $\delta\mathbf{H}$ depending on the local velocity $\mathbf{U}$. If the perturbation is small the new solution will remain periodic but with a different period (in contrast with the corresponding linear problem whose frequency will in general become complex and bring about either amplification or damping). In order to be able to treat the problem perturbatively and avoid secular effects, it is convenient to scale the time variable on the period of the solution itself. Thus introducing the scaled time

$$\tau = \frac{t}{T} \tag{30}$$

the perturbed equations can be rewritten as

$$\frac{1}{T}\frac{\partial \mathbf{U}}{\partial \tau} + \mathbf{U}\cdot\nabla\mathbf{U} = -\nabla P + \frac{1}{Re}\boldsymbol{\Delta}\mathbf{U} + \delta\mathbf{H}(\mathbf{U}) \tag{31a}$$

$$\nabla\cdot\mathbf{U} = 0 \tag{31b}$$

where T is an additional unknown and the period in the variable τ is constant and equal to 1.

Writing the perturbed solution as

$$\{\mathbf{U}(x,y,\tau), P(x,y,\tau)\} = \{\mathbf{U}_b(x,y,\tau) + \mathbf{u}(x,y,\tau), P_b(x,y,\tau) + p(\tau)\}, \tag{32}$$

where $\mathbf{Q_b} \equiv \{\mathbf{U_b}, P_b\}$ denotes the unperturbed periodic flow and $\mathbf{q} \equiv \{\mathbf{u}, p\}$ have become the small perturbations induced by the added forcing, and inserting it into the equations together with the small external forcing $\delta\mathbf{H}(\mathbf{U}) = \mathbf{C}(x,y)\ \mathbf{U}(x,y,\tau)$ we obtain

$$\frac{1}{T+\delta T}\frac{\partial(\mathbf{U_b}+\mathbf{u})}{\partial\tau} + (\mathbf{U_b}+\mathbf{u})\cdot\nabla(\mathbf{U_b}+\mathbf{u}) + \nabla(P_b+p) = \frac{1}{Re}\boldsymbol{\Delta}(\mathbf{U_b}+\mathbf{u}) + \delta\mathbf{H}(\mathbf{U_b}+\mathbf{u}) \tag{33a}$$

$$\nabla\cdot(\mathbf{U_b}+\mathbf{u}) = 0 \tag{33b}$$

Downloaded by Gurlith Petersson on November 7, 2012 | http://arc.aiaa.org | DOI: 10.2514/6.2008-4227

If the effect of the structural perturbation is small, we can linearise these equations and obtain an equation for the perturbation

$$\frac{1}{T}\frac{\partial \mathbf{u}}{\partial \tau} + \mathbf{L}\{\mathbf{U}_b, Re\}\ \mathbf{u} + \nabla p = \frac{\delta T}{T^2}\frac{\partial \mathbf{U_b}}{\partial \tau} + \delta \mathbf{H}(\mathbf{U}_b) \tag{34a}$$

$$\nabla \cdot \mathbf{u} = 0 \tag{34b}$$

where $\mathbf{L}\{\mathbf{U}_b, Re\}$ is the two-dimensional Linearised Navier–Stokes operator defined by (5). This linear problem can be studied through Floquet analysis, and, as is well known, the resulting perturbation will in general *not* be periodic, but modified by the Floquet exponent. The condition, implicit in the definition of τ, that a constant period equal to 1 be maintained, constitutes a compatibility condition determining δT, which is exactly the variation of period induced by the structural perturbation $\delta \mathbf{H} = \mathbf{C}\mathbf{U_b}$.

Just as in the corresponding linear stability problem, we can obtain the sensitivity of the period to an *arbitrary* structural perturbation with the aid of adjoint equations. The key to this approach is the observation that the unperturbed equations (31) have a non-unique solution, insofar as if $\mathbf{U_b}(x, y, \tau)$ is a periodic solution, $\mathbf{U_b}(x, y, \tau + \delta\tau)$ is as well. Linearising with respect to $\delta\tau$ we find that $\partial \mathbf{U_b}/\partial\tau$ is a solution of the linearised equations (34) in homogeneous form (*e.g.*, with $\delta\mathbf{H} = 0$). Since equations (34) with periodic boundary conditions have a nontrivial solution with zero forcing and zero δT, the original inhomogeneous linear problem only has a solution if a compatibility condition is satisfied. This compatibility condition can be derived exploiting the adjoint equations. Note in particular that (33) is a linear partial differential equation of the same form as (21) but with $\kappa = 0$, $\delta\mathbf{R} = 0$ and $\delta\sigma = 0$. Thus we can use equations (23) to derive the compatibility conditions: in particular taking $\delta\sigma = 0$ and using $\frac{\delta T}{T^2}\frac{\partial \mathbf{U_b}}{\partial \tau} + \delta\mathbf{H}(\mathbf{U}_b)$ as forcing term we easily obtain

$$N\frac{\delta T}{T} = -\int_t^{t+T}\int_{\mathcal{D}} \mathbf{f}^+ \cdot \mathbf{C} \cdot \mathbf{U_b}\ \mathrm{d}^2\mathbf{x}\,\mathrm{d}t \quad \text{where} \quad N = \int_t^{t+T}\int_{\mathcal{D}} \mathbf{f}^+ \cdot \frac{\partial \mathbf{U_b}}{\partial \tau}\ \mathrm{d}^2\mathbf{x}\,\mathrm{d}t \tag{35}$$

where $\mathbf{f}^+$ represents the neutral adjoint eigenfunction corresponding to the Floquet exponent $\sigma = 0$. If we now assume a feedback of the form (25), i.e. a feedback localised in space, the previous expression can be further simplified. In particular noting that $\delta\omega/\omega = -\delta T/T$, we easily obtain the structural sensitivity $\mathbf{S}$ of the oscillation frequency ω to a localised feedback $\mathbf{C}_0$ as

$$\mathbf{S} = \frac{\delta\omega}{\delta\mathbf{C}} = \frac{\omega}{N}\int_t^{t+T} \mathbf{U_b}\ \mathbf{f}^+\ \mathrm{d}t \tag{36}$$

As in the linear case, the notation $\mathbf{U_b}\ \mathbf{f}^+$ must be read as a dyadic product.

V.A. Numerical Results and comparison with the linear results

Giannetti, Pralits & Luchini (2007)[13] and Luchini, Pralits & Giannetti (2008)[14] numerically determined, for different Reynolds numbers, both the periodic base solution and the adjoint field $\mathbf{f}^+$ by numerically integrating the two-dimensional nonlinear and adjoint equations (2) and (12). For spatial discretization a classical finite difference scheme was adopted. An immersed boundary was used to easily represents the effects of the cylinder on a Cartesian mesh. The advancement in time was obtained by a classical third order mixed Runge-Kutta Crank-Nicolson scheme. The periodic base flow and the adjoint field were determined by letting the corresponding equations evolve in time until a periodic state was found. As in the linear case, in order to localise the region of high sensitivity, a spatial map was built by taking at each point of the domain a given norm of the sensitivity tensor.

Figure 4 shows a typical result obtained using this approach: a space distribution of the structural sensitivity $\mathbf{S}$ defined by equation (36) at $\Re = 50$,a slightly unstable configuration. The white line in the figure indicates the recirculation bubble of the mean flow. As $\mathbf{S}$ is a tensor, various representative quantities may be used to generate the sensitivity map. Here the spectral norm of $\mathbf{S}$ was used, but other choices are equally possible. For this case, however, both the spectral or the Frobenius norm and the modulus of the trace of $\mathbf{S}$ gave almost identical results. The region of high sensitivity is located in two narrow strips starting close to the separation point of the mean flow and extending downstream for a few diameters. Results for $Re = 60$, 80, 100 and 150 are shown in figure 5. Note that as the Reynolds number is increased the region of high sensitivity shortens and at the same time bends and tends to close.

Downloaded by Gurlith Petersson on November 7, 2012 | http://arc.aiaa.org | DOI: 10.2514/6.2008-4227

Downloaded by Gurlith Petersson on November 7, 2012 | http://arc.aiaa.org | DOI: 10.2514/6.2008-4227

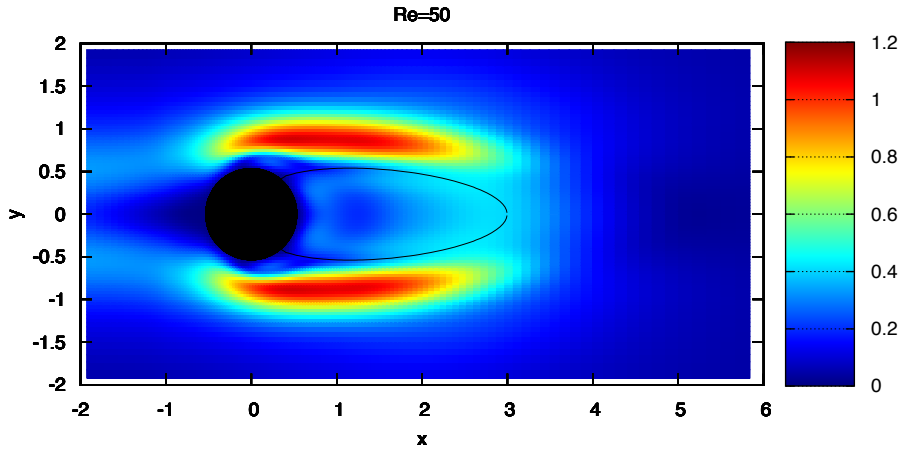

Figure 4. Structural sensitivity of the periodic wake at Re=50: sensitivity to a local force depending on the local value of the velocity of the worst direction ($\|S\|_2$)

V.B. Comparison with the linear results

The results obtained through this analysis agree remarkably well with the experimental data of Strykowski & Sreenivasan (1990),[15] who introduced a small perturbing cylinder in the wake of a larger one and reported the variation in critical Reynolds number as a function of position of the perturbing cylinder (figure 6). It is however a surprise that the structural sensitivity of the saturated periodic oscillation, even at the relatively low Reynolds number of 50, does not agree as satisfactorily with the structural sensitivity of the linear eigenmode as calculated by Giannetti & Luchini (2007)[3] and displayed in figure 2). Actually, if attention is paid to the colour scale, it will be seen that the two are quite different in amplitude and not just in shape. This was a puzzle until we realized that the frequency of the nonlinear oscillation can be influenced in two different ways: by a structural perturbation force determined by the fluctuating velocity alone (as implicitly assumed in our linear results), or by a force that responds both to the mean and to the fluctuating velocity. Neither is wrong: they serve different purposes. The structural perturbation depending on the fluctuation only was the appropriate tool to study the position of the *wavemaker*, but the perturbation depending on the full velocity field is the one that was implicitly assumed in the present nonlinear results, and of course is the one that occurs in the experiments. Once this difference is identified, it is not difficult to extend the linear eigenmode calculation to account for the frequency variation induced by a perturbation influencing the base flow. As an example, figure 7 shows the total sensitivity (the spectral norm is used to generate the map) of the linear instability mode, *i.e.* the sum of the sensitivities to a base-flow modification induced by a spatially localised feedback acting at base flow level and to a spatially localised feedback acting at the perturbation level. It is now evident that a more satisfactory agreement is recovered with both experiments and nonlinear sensitivity results.

In other terms this outcome clearly reveals that the mean-flow modification induced by a small perturbing body is responsible for a much larger effect than the direct influence of the perturbing body on the oscillation. This important information show that the analysis based on the structural sensitivity approach may represent a powerful tool in the design of effective control strategies. The identification of the different contributions to the total sensitivity also suggest an easy way to identify the wavemaker of the nonlinear state. The core of the instability in fact can be localised by evaluating the sensitivity of the nonlinear periodic oscillation to a zero-mean feedback. This is done by subtracting from the previous calculations the effects of the mean-flow modifications. Figures 8 and 9 show the results obtained by replacing in 35 $\mathbf{U_b}$ with $\mathbf{U_b} - \bar{\mathbf{U}}_\mathbf{b}$, where $\bar{\mathbf{U}}_\mathbf{b}$ is

Downloaded by Gurlith Petersson on November 7, 2012 | http://arc.aiaa.org | DOI: 10.2514/6.2008-4227

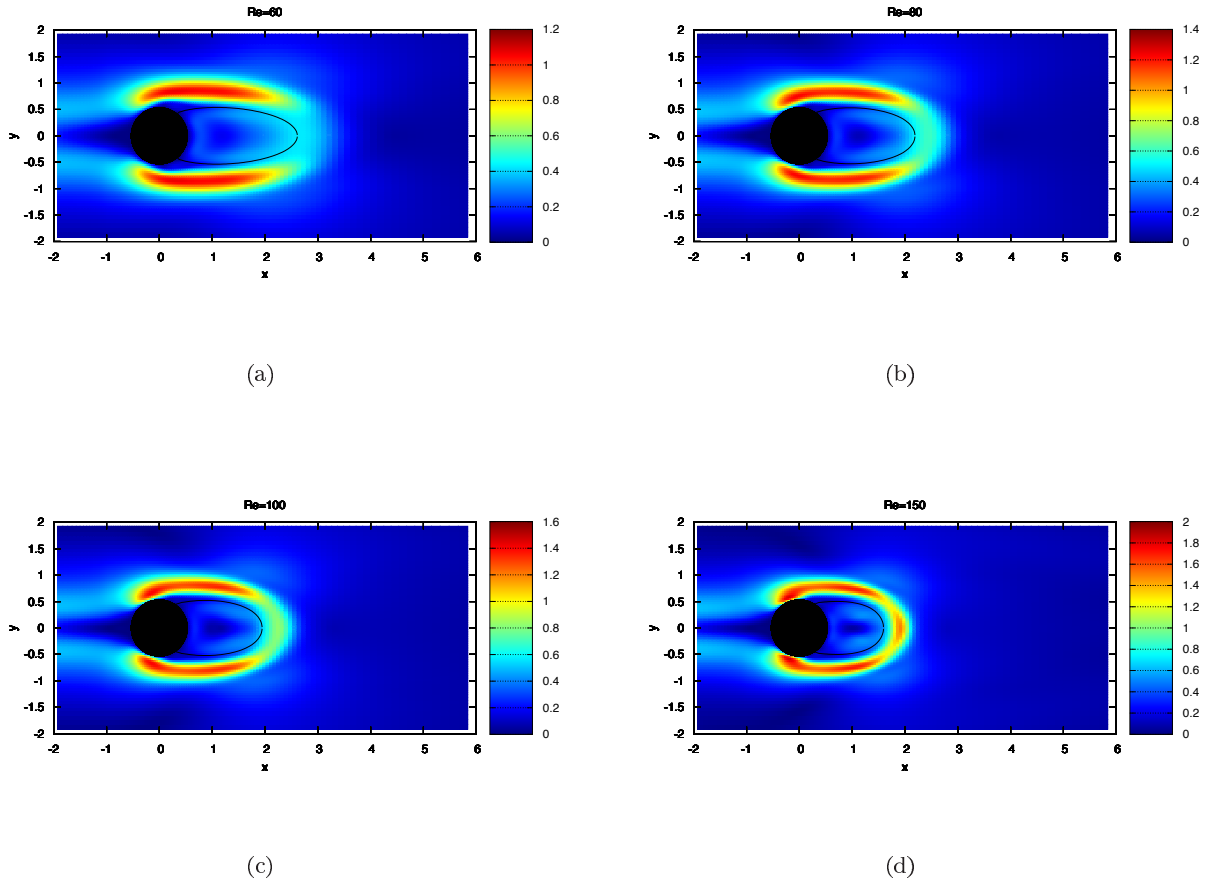

Figure 5. Spatial distribution of the spectral norm of the sensitivity tensor S: (a) $Re = 60$, (b) $Re = 80$, (c) $Re = 100$,(d) $Re = 150$

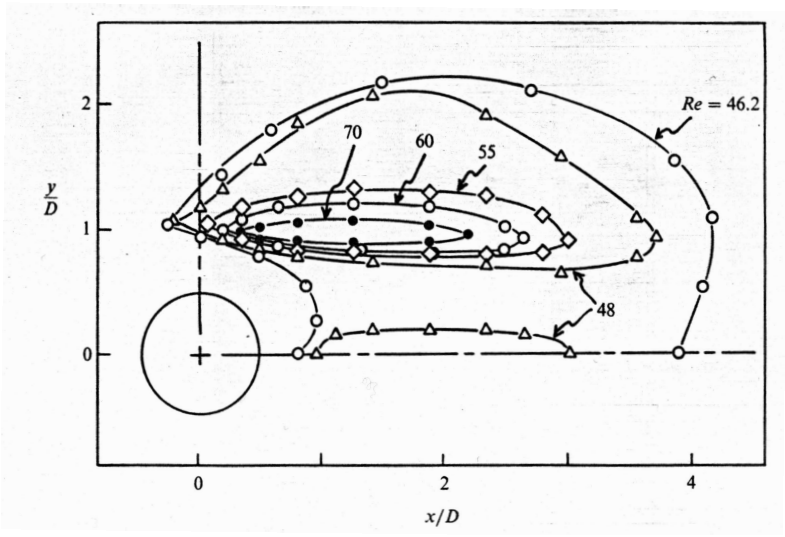

Figure 6. Experiment of Strykowski & Sreenivasan (1990)

the average value of $\mathbf{U_b}$ over a shedding period. The resulting maps may now be compared with their linear equivalent (2) and (3). It can be observed that close to the critical Reynolds number $Re_{c,1}$ the region where

Downloaded by Gurlith Petersson on November 7, 2012 | http://arc.aiaa.org | DOI: 10.2514/6.2008-4227

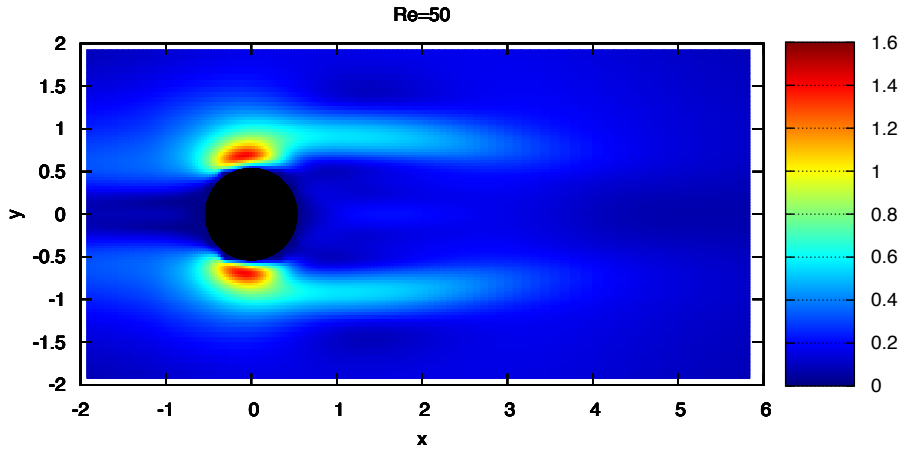

Figure 7. Structural sensitivity of the linear instability mode at Re=50 with base-flow modifications included (the spectral norm).

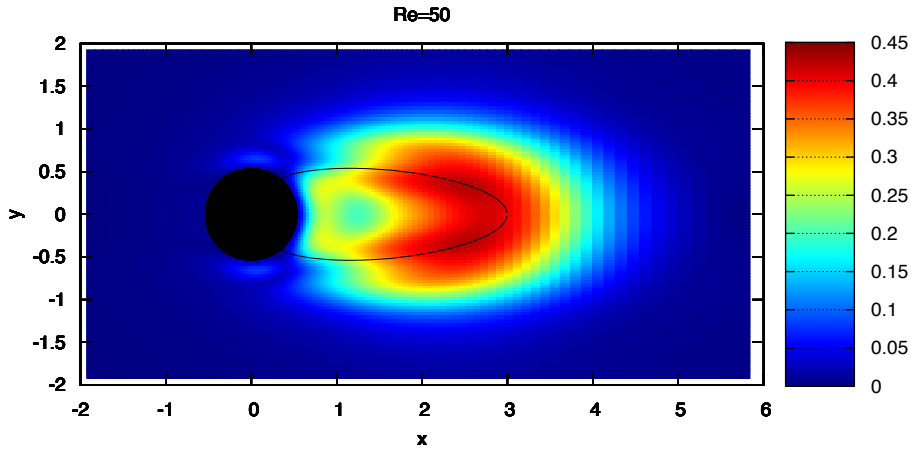

Figure 8. Sensitivity of the periodic oscillation to a zero-mean feedback at Re=50 ($\|S\|_2$)

the sensitivity is large is similar to that obtained through a linear analysis of the steady unstable base flow. This is understood by considering that the mean flow and the unstable basic state are, in that case, quite similar. An even better agreement, at least for what concerns the shape of the region of high sensitivity, can be recovered if the effects of the phase shift are taken into account. This can be achieved by considering the spatial distribution of the function

Downloaded by Gurlith Petersson on November 7, 2012 | http://arc.aiaa.org | DOI: 10.2514/6.2008-4227

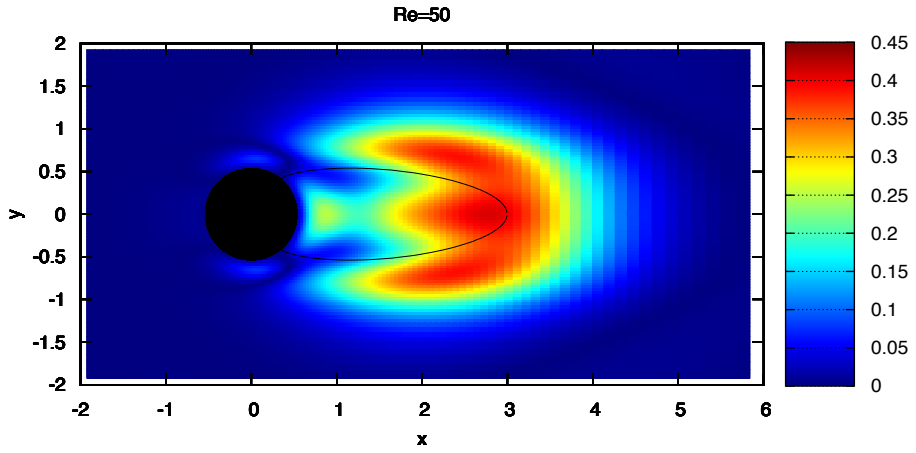

Figure 9. Sensitivity of the periodic oscillation to a zero-mean feedback at Re=50 ($|\mathrm{Tr}(\mathbf{S})|$)

$$\lambda(x,y) = \frac{\omega}{N}\int_t^{t+T} \|\mathbf{U_b}(x,y)\ \mathbf{f}^+(x,y)\|_2\ \mathrm{d}t \tag{37}$$

which represent the sensitivity to a spatially localised feedback in which the force depends on a local velocity that takes the worst possible direction at each instant in time. As an example, figure 11 shows the spatial map obtained from (37): the shape of the region of maximum sensitivity is now in excellent agreement with that depicted in figure 2.

As the Reynolds number is increased, the shape of the sensitivity map changes and the location of the *wavemaker* moves toward the end of the recirculation bubble of the mean flow $\bar{\mathbf{U}}_\mathbf{b}$. This behaviour is displayed in figure 10 in which the spatial sensitivity maps for $Re = 60$, 80, 100 and 150 are displayed. In order to confirm these results a linear stability analysis was also performed on the mean-flow. It is well known in fact that the imaginary part of the eigenvalue σ of the corresponding linear stability problem well approximates the real shedding frequency of the periodic solution. It is therefore reasonable to suppose that for this flow a structural sensitivity analysis of the mean-flow can be used to identify the location of nonlinear wavemaker. As an example figure 12 displays the spectral norm of the sensitivity tensor obtained by a linear stability analysis of the mean flow. The qualitative agreement with figure 10 (d) is satisfactory and confirms the validity of the nonlinear approach.

VI. Structural sensitivity of the secondary instabilities

Although the approach based on the structural sensitivity analysis was originally developed to fully understand the first instability of the cylinder wake and to locate the "wavemaker" of the asymptotic theory, a similar approach can also be used to study the characteristics of the secondary instability. It is well known in fact that the two-dimensional time-periodic Kármánstreet described in the previous section becomes unstable to three-dimensional perturbations when the Reynolds number exceeds a critical threshold of $Re_{c,2} \approx 189$. The secondary instability of the wake of a circular cylinder is a well known phenomenon and has been widely studied in the last two decades (see, for instance, Barkley *et al.* (1999),[16] Barkley & Henderson (1996)[6] and Williamson (1996)[8]). A Floquet linear stability analysis shows the existence of two separate bands of synchronous unstable modes: the first one (mode A) appears at $Re \simeq 189$ and is characterised by a spanwise wavelength of about 4 cylinder diameters, while the second one (mode B) develops for $Re > 259$ and has

Downloaded by Gurlith Petersson on November 7, 2012 | http://arc.aiaa.org | DOI: 10.2514/6.2008-4227

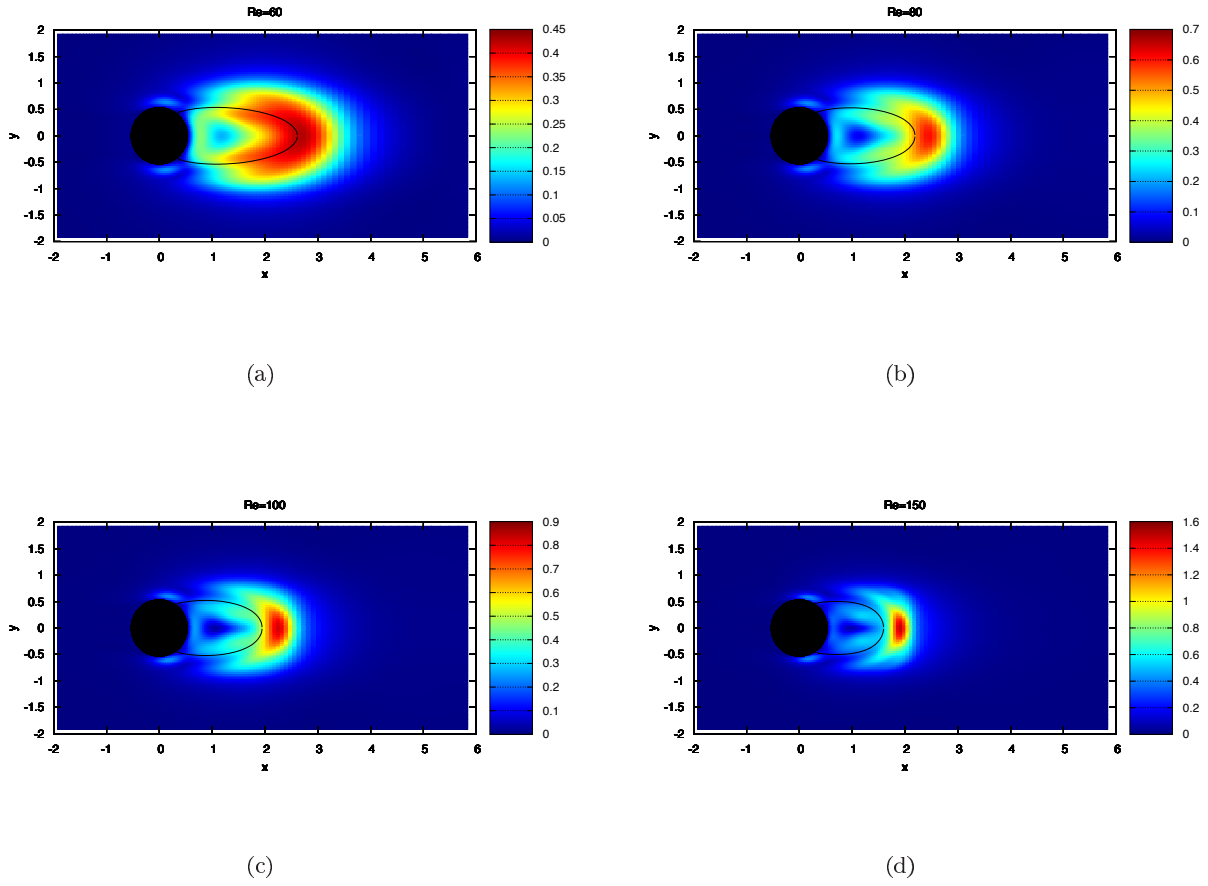

(a) (b)

(c) (d)

Figure 10. Sensitivity of the periodic oscillation to a zero-mean feedback ($\|\mathbf{S}\|_2$): (a) $Re = 60$, (b) $Re = 80$, (c) $Re = 100$,(d) $Re = 150$

a shorter spanwise length-scale (about 1 diameter). Several physical mechanisms have been proposed to explain this transition to a three-dimensional flow. Some authors, for example (see Thompson *et al.* 2001[17]), suggested that mode A is related to an elliptic instability of the vortex cores of the Kármánstreet, while mode B is associated with an instability of the braid region between the rollers .

More recently, Barkley (2005),[18] carrying out the Floquet stability analysis on several restricted subdomains, showed that only a small region of the flow behind the cylinder plays a role in the development of the secondary instability. A similar behaviour was also observed by Giannetti & Luchini (2007)[3] in the study of the first instability (see section IV.A) and successfully explained in terms of structural sensitivity. Giannetti, Camarri & Luchini (2008)[19] generalised this approach by extending its applicability to three-dimensional problems with a periodic time-dependent base flow. In this way they arrived to the general formulation presented in section III. Such approach, being the most general, can be used to recover the original results of Giannetti & Luchini (2007)[3] (as shown in section IV) or to derive the compatibility condition for the nonlinear approach (described in section V), but can also be applied to study the structural sensitivity of the secondary instability of the cylinder wake. The key to this analysis resides again in formula (VI) which defines the sensitivity tensor for a spatially localised feedback as

$$\mathbf{S}(x,y) = \frac{\delta\sigma}{\delta\mathbf{C}_0} = \frac{\displaystyle\int_t^{t+T} \hat{\mathbf{u}}(x,y,\kappa,t)\ \hat{\mathbf{f}}^{+}(x,y,\kappa,t)\ \mathrm{d}t}{\displaystyle\int_t^{t+T}\int_{\mathcal{D}} \hat{\mathbf{f}}^{+}\cdot\hat{\mathbf{u}}\ \mathrm{d}^2\mathbf{x}\ \mathrm{d}t} \quad .$$

Note that in contrast with the two-dimensional cases treated in the previous sections, the sensitivity tensor

Downloaded by Gurlith Petersson on November 7, 2012 | http://arc.aiaa.org | DOI: 10.2514/6.2008-4227

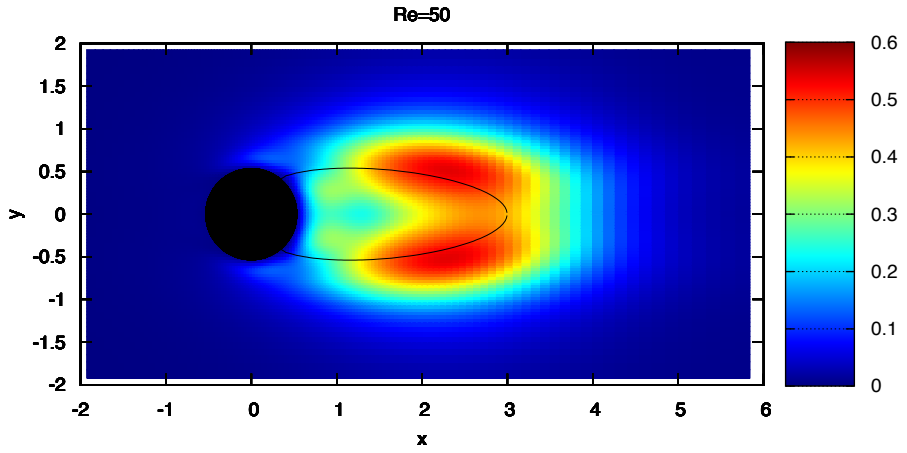

Figure 11. Spatial distribution of the function $\lambda(x, y)$ at Re=50

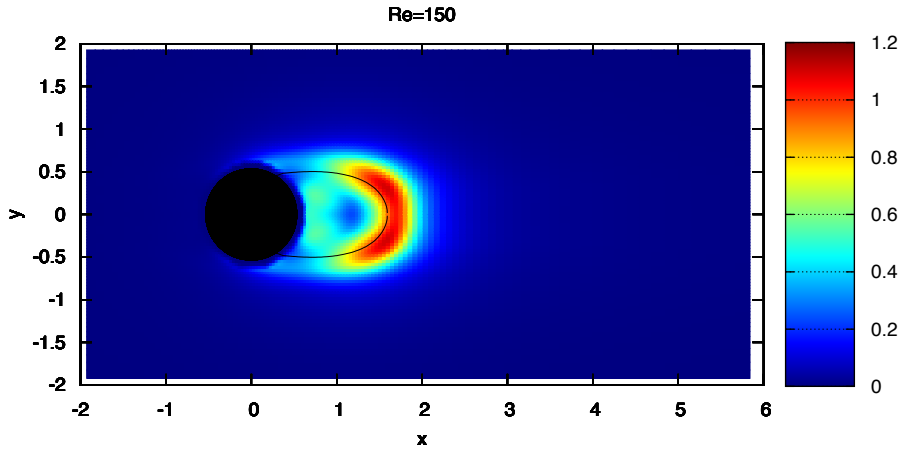

Figure 12. Structural sensitivity obtained through a linear stability analysis of the mean flow $\bar{\mathrm{U}}_b$ at Re=150

is now represented by a 3 by 3 matrix. The stability characteristics of the flow for a given value of κ and Re can be numerically determined by finding the first eigenvalues of the Floquet transition operator (*i.e.* the Floquet exponents σ). This can be achieved by using a simple power iteration or more efficiently through the implementation of an Arnoldi-type iteration. After the evaluation of both the direct and the adjoint Floquet modes corresponding the unstable exponent it is possible to determine all the components of the tensor $\mathbf{S}$ and consequently build a spatial sensitivity map. This has been recently achieved by Giannetti, Camarri

& Luchini (2008): as an example of their results, figure (13) shows the spatial maps obtained by plotting locally the value of the spectral norm of S, respectively for mode A at $Re = 200$ and mode B at $Re = 259$. It can be noticed that in both cases the instability is highly localised and confined in a region of the wake very close to the cylinder surface. In order to validate the results, following Barkley, a Floquet stability analysis was performed on several restricted domains. The results of this analysis confirmed that a non-negligible drift of the Floquet exponent is obtained only when the computational domain does not contain the whole region of high sensitivity depicted in figure 13. According to these results the characteristics of mode A and B are dictated by the conditions of different regions of the flow. Note in fact that while the sensitivity of mode A is concentrated in a single patch located across the symmetry line, the sensitivity of mode B attains its maximum in two small regions symmetrically placed and split apart by a distance of about one diameter. Note also that sensitivity of mode B is much larger than that of mode A.

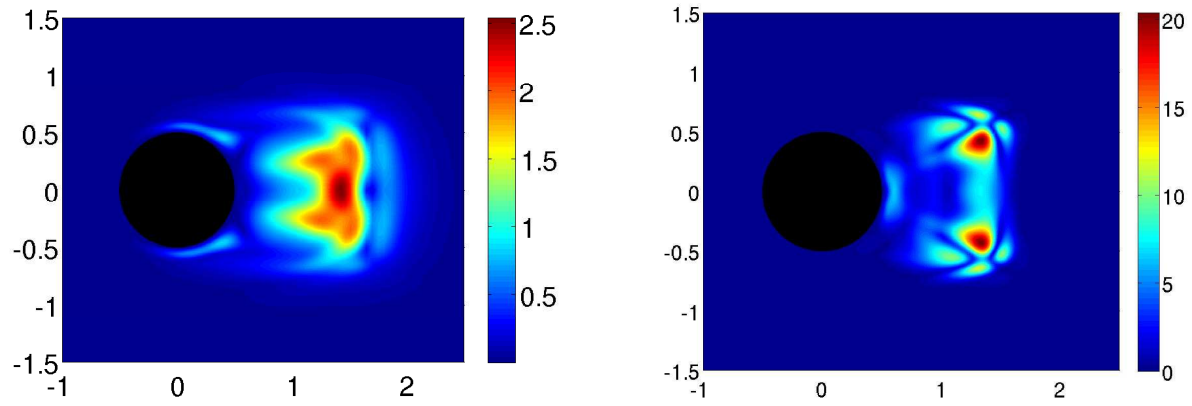

(a) Mode A

(b) Mode B

Figure 13. Sensitivity map (spectral norm) of the Floquet exponent to structural perturbations of the Floquet transition operator: (a) mode A at $Re = 200$ and wavenumber $k = 1.6$; (b) mode B at $Re = 259$ and wavenumber $k = 7.6$.

More insights in the development of the secondary instability can be retrieved by inspecting the time evolution of the integrand of equation (VI). For example figures 14 and 15 shows the time evolution of the function

$$s(x, y, \kappa, t) = \frac{\|\mathbf{f}^{+}(x, y, \kappa, t)\ \mathbf{u}(x, y, \kappa, t)\|_2}{\int_t^{t+T} \int_{\mathcal{D}} \hat{\mathbf{f}}^{+} \cdot \hat{\mathbf{u}}\ \mathrm{d}S\ \mathrm{d}t} \quad . \tag{38}$$

over a shedding cycle respectively for mode A and mode B.

These results reveal that, both for mode A and B, the regions of high sensitivity evolve in time with a rather complex behaviour, showing an even more localised structure. A more detailed analysis which tries to link the properties of the sensitivity tensor to local characteristics of the periodic base flow is actually in progress and might help to shed a new light on the nature of the secondary instability or to develop effective control strategies for its suppression.

VII. Conclusion

In this paper we review the concept of "structural sensitivity" and show how such notion may be used to study the characteristics of the global instabilities arising in the wake of bluff bodies. In particular, by looking at the structural sensitivity of the linear unstable global mode it is possible to locate the "wavemaker", *i.e.*the position in which, according to the asymptotic theory, the instability originates and from which it propagates in all direction. The original formulation introduced by Giannetti & Luchini (2007)[3] is extended to treat three-dimensional perturbations evolving on a time-periodic base flow and applied to study the finite-amplitude vortex shedding behind a circular cylinder. By comparing the new results with those obtained by Giannetti & Luchini (2007)[3] it is found that the total sensitivity is composed by two different contributions: the direct effect of the feedback on the nonlinear oscillation and the effect of the mean-flow modification induced by the structural perturbation. Such information is used to locate the nonlinear wavemaker, which is

Downloaded by Gurlith Petersson on November 7, 2012 | http://arc.aiaa.org | DOI: 10.2514/6.2008-4227

Downloaded by Gurlith Petersson on November 7, 2012 | http://arc.aiaa.org | DOI: 10.2514/6.2008-4227

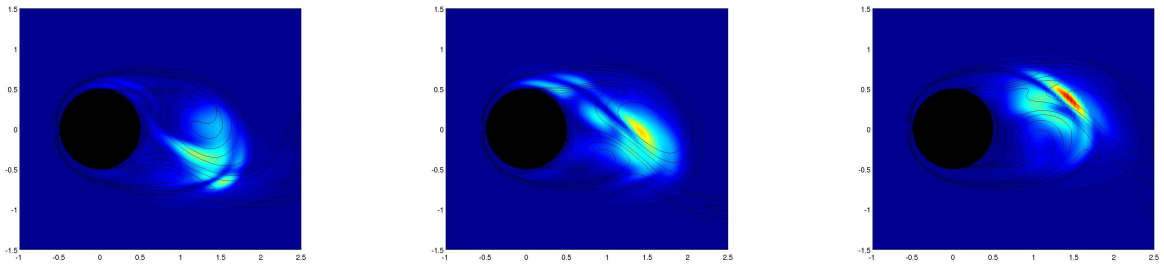

(a) $t = 0$ (b) $t = \frac{1}{6}T$ (c) $t = \frac{2}{6}T$

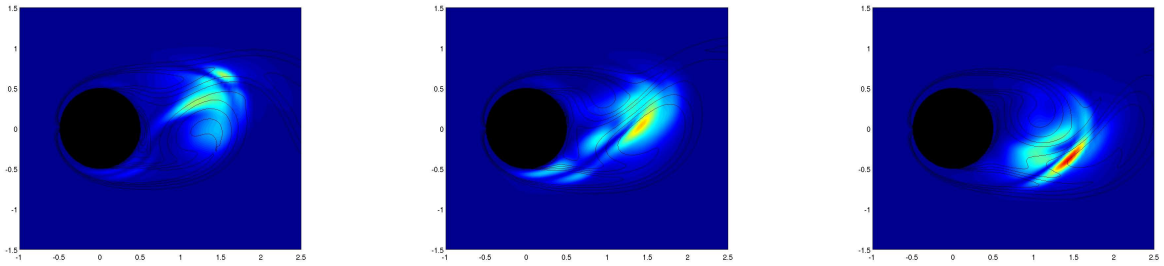

(d) $t = \frac{3}{6}T$ (e) $t = \frac{4}{6}T$ (f) $t = \frac{5}{6}T$

Figure 14. Time evolution of the function $s(x, y, \kappa, t)$ for mode A ($Re = 200$, $\kappa = 1.6$)

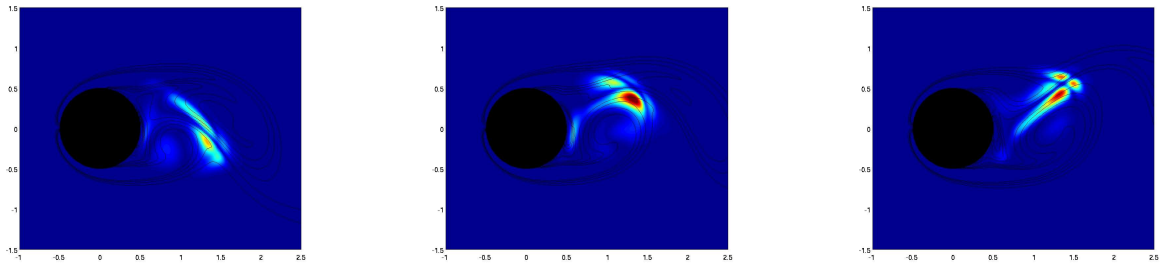

(a) $t = 0$ (b) $t = \frac{1}{6}T$ (c) $t = \frac{2}{6}T$

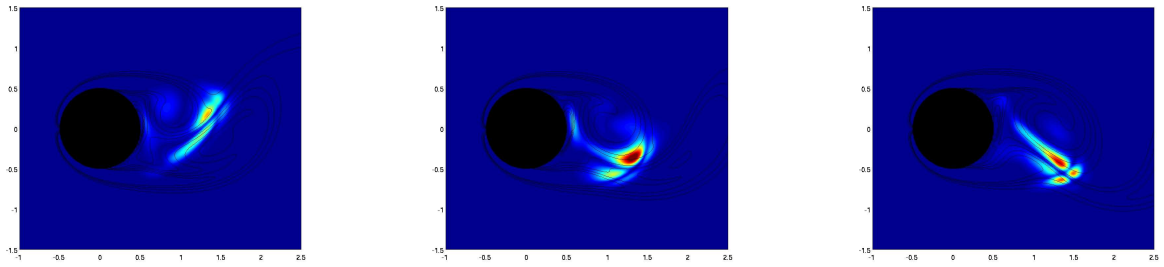

(d) $t = \frac{3}{6}T$ (e) $t = \frac{4}{6}T$ (f) $t = \frac{5}{6}T$

Figure 15. Time evolution of the function $s(x, y, \kappa, t)$ for mode B ($Re = 259$, $\kappa = 7.6$)

identified by plotting the sensitivity to a zero-mean feedback. Finally, the concept of structural sensitivity is applied to study the characteristics of the secondary instabilities of the cylinder wake. Following Giannetti, Camarri & Luchini (2008),[19] a Floquet stability analysis is performed to determine both the direct and adjoint unstable Floquet modes. The structural sensitivity to spatially localised feedbacks is then evaluated

both for mode A and B, showing that such instabilities are extremely localised in space.

References

[1]Huerre, P. and Monkewitz, P. A., "Local and global instabilities in spatially developing flows," *Ann. Rew. Fluid Mech.*, Vol. 22, 1990, pp. 473–537.

[2]Chomaz, J.-M., "Global Instabilities in Spatially Developing Flows: Non-Normality and Nonlinearity," *Ann. Rew. Fluid Mech.*, Vol. 156, 2005, pp. 209–240.

[3]Giannetti, F. and Luchini, P., "Structural sensitivity of the first instability of the cylinder wake," *J. Fluid Mech.*, Vol. 581, 2007, pp. 167–197.

[4]Provansal, M., Mathis, C., and Boyer, L., "Bénard-von Kármán instability: transient and forced regimes," *J. Fluid Mech.*, Vol. 182, 1987, pp. 1–22.

[5]Noack, B. R. and Eckelmann, H., "A global stability analysis of the steady and periodic cylinder wake," *J. Fluid Mech.*, Vol. 270, 1994, pp. 297–330.

[6]Barkley, D. and Henderson, R., "Three-dimensional Floquet stability analysis of the wake of a circular cylinder," *J. Fluid Mech.*, Vol. 322, 1996, pp. 215–241.

[7]Williamson, C. H. K., "Defining a universal and continuous Strouhal-Reynolds number relationship for the laminar vortex shedding of a circular cylinder," *Phys. Fluids*, Vol. 31, 1988, pp. 2742–2744.

[8]Williamson, C. H. K., "Vortex dynamics in the cylinder wake," *Ann. Rew. Fluid Mech.*, Vol. 28, 1996, pp. 477–539.

[9]Chomaz, J.-M., Huerre, P., and Redekopp, L., "A frequency selection criterion in spatially developing flows," *Stud. Appl. Maths*, Vol. 84, 1991, pp. 119–144.

[10]Monkewitz, P. A., Huerre, P., and Chomaz, J.-M., "Global linear stability analysis of weakly non-parallel shear flows," *J. Fluid Mech.*, Vol. 251, 1993, pp. 1–20.

[11]Le Dizès, S., Huerre, P., Chomaz, J.-M., and Monkewitz, P. A., "Linear global modes in spatially developing media," *Phil. Trans. R. Soc. Lond.*, Vol. 354, 1996, pp. 169–212.

[12]Triantafyllou, G. S. and Karniadakis, G. E., "Computational reducibility of unsteady viscous flows," *Phys. Fluids A*, Vol. 2, 1990, pp. 653–656.

[13]Giannetti, F., Pralits, J. O., and Luchini, P., "Structural sensitivity of the finite-amplitude vortex shedding behind bluff bodies," *Proc. 18th Congress of the Italian Association of Theoretical and Applied Mechanics (AIMETA), 11-14 September 2007, Brescia, Italy*, 2007.

[14]Luchini, P., Pralits, J. O., and Giannetti, F., "Structural sensitivity of the finite-amplitude vortex shedding behind a circular cylinder," *Proc. IUTAM Symposium on unsteady separated flows and their control, 18-22 June 2007, Corfu, Greece*, Springer, 2008.

[15]Strykowski, P. J. and Sreenivasan, K. R., "On the formation and suppression of vortex "shedding" at low Reynolds number," *JFM*, Vol. 218, 1990, pp. 71–107.

[16]Barkley, D., Tuckerman, L. S., and Golubitsky, M., "Bifurcation theory for three-dimensional flow in the wake of a circular cylinder," *Physical Review E*, Vol. 61, 1999, pp. 5247–5252.

[17]Thompson, M. C., Leweke, T., and Williamson, C. H. K., "The mechanism of transition in bluff body wake," *Journal of Fluids and Structures*, Vol. 15, 2001, pp. 607–616.

[18]Barkley, D., "Confined three-dimensional stability analysis of the cylinder wake," *Physical Review E*, Vol. 71, 2005, pp. 017301.

[19]Giannetti, F., Camarri, S., and Luchini, P., "Structural sensitivity of the secondary instability of the cylinder wake," In preparation.

Downloaded by Gurlith Petersson on November 7, 2012 | http://arc.aiaa.org | DOI: 10.2514/6.2008-4227